

The Stagnation Hugoniot Analysis for Steady Combustion Waves in Propulsion Systems

E. Wintenberger*, and J.E. Shepherd[†]

Graduate Aeronautical Laboratories,

California Institute of Technology, Pasadena, CA 91125

Revised October 13, 2005

The combustion mode in a steady-flow propulsion system has a strong influence on the overall efficiency of the system. In order to evaluate the relative merits of different modes, we propose that it is most appropriate to keep the upstream stagnation state fixed and the wave stationary within the combustor. Due to the variable wave speed and upstream stagnation state, the conventional Hugoniot analysis of combustion waves is inappropriate for this purpose. To remedy this situation, we propose a new formulation of the analysis of stationary combustion waves for a fixed initial stagnation state, which we call the stagnation Hugoniot. For a given stagnation enthalpy, we find that stationary detonation waves generate a higher entropy rise than deflagration waves. The combustion process generating the lowest entropy increment is found to be constant-pressure combustion. These results clearly demonstrate that the minimum entropy property of detonations derived from the conventional Hugoniot analysis does not imply superior performance in all propulsion systems. This finding reconciles previous analysis of flow path performance analysis of detonation-based ramjets with the thermodynamic cycle analysis of detonation-based propulsion systems. We conclude that the thermodynamic analysis of propulsion systems based on stationary detonation waves must be formulated differently than for propagating waves, and the two situations lead to very different results.

*now at GE Advanced Materials Quartz, Strongsville, OH 44149

[†]Professor, Aeronautics, Member AIAA

Nomenclature

a_f	flow availability per unit mass
C_p	specific heat capacity at constant pressure
F	thrust
h	enthalpy per unit mass
h_0^r	enthalpy per unit mass of reactants at environment conditions
h_0^p	enthalpy per unit mass of products at environment conditions
h_t	total enthalpy per unit mass
M	Mach number
\dot{m}	mass flow rate
P	pressure
P_0	pressure of the environment
P_t	total pressure
\dot{P}_s	entropy generation per unit time
q_c	heat of combustion per unit mass of mixture
q_{in}	heat per unit mass input into the system during a cycle
q_{out}	heat per unit mass removed from the system during a cycle
R	perfect gas constant
s	entropy per unit mass
s_0^r	entropy per unit mass of reactants at environment conditions
s_0^p	entropy per unit mass of products at environment conditions
T	temperature
T_0	temperature of the environment
T_t	total temperature
u	flow velocity in fixed reference frame
u'	flow velocity in wave reference frame
v	specific volume
w	work per unit mass
\dot{w}_{ideal}	ideal work per unit time
γ	specific heat ratio
Δs_{irr}	irreversible part of entropy rise
Δs_{min}	minimum part of entropy rise
Δs_{rev}	reversible part of entropy rise
ρ	density
η_{th}	thermal efficiency

Introduction

A key issue in conceptual design and analysis of proposed propulsion systems is the role of the combustion mode in determining the overall efficiency of the system. Because entropy production is detrimental to the efficiency of propulsion systems,¹ optimizing a propulsion system means minimizing the overall entropy generation in the flow. The entropy increment associated with the combustion process is often the largest of all increments through the propulsion system. This is why the selection of the combustion mode is critical to engine performance.

Chapman-Jouguet (CJ) detonation waves are of particular interest since they apparently correspond to the minimum entropy generation² of all combustion wave modes. This result, along with the similarities between detonation and constant-volume combustion, has often been quoted in the literature as a motivation to explore detonation applications to propulsion.³⁻⁵ On a thermodynamic basis, idealized unsteady propulsion systems based on propagating detonations appear to have the potential for high efficiency. However, the situation appears to be the opposite for steady-flow propulsion systems based on stationary detonation waves in spite of the apparent lower entropy rise generated by detonations as compared with deflagrations. The performance⁶⁻⁸ of steady detonation-based engines is systematically and substantially lower than that of the deflagration-based engines.

These results are in agreement with the early work of Zel'dovich⁹ and Foa^{3,10} on steady-flow propulsion. Looking at a detonation wave as a shock wave followed by a reaction zone, Zel'dovich qualitatively argued that this process generates more entropy than a deflagration, and estimated the thrust reduction associated with the use of a detonation wave instead of a deflagration in an air-breathing jet engine.⁹ Foa concluded¹⁰ that, in a constant-area burner, constant-pressure combustion is the optimal combustion mode using a polytropic representation of the combustion process. He also recognized³ that, in steady-flow propulsion systems, the type of combustion mode is constrained by the requirement for a stationary reaction front, and that combustion modes should be compared for a fixed stagnation temperature. On this basis, Foa compared a subsonic-combustion ramjet and a detonation-based ramjet and concluded that subsonic combustion produced a lower entropy rise than steady detonation.³

The differing results for steady-flow and propagating detonation propulsion system analysis lead us to re-examine the conventional Hugoniot analysis and the minimum entropy property of the CJ point. In doing so, it is important to distinguish between using propagating detonation waves in an unsteady cycle, as in a pulse detonation engine, and stationary waves in a steady cycle, as in a detonation ramjet or oblique detonation engine. Despite the common feature of detonation, the boundary conditions for the combustor are completely

different for the two applications, and the nature of the cycle is completely different. In pulse detonation engines, an unsteady, cyclic thermodynamic analysis with a propagating detonation wave is appropriate. In a detonation ramjet, a steady open-system thermodynamic analysis with a stationary detonation wave is appropriate. In the present paper, we focus exclusively on the steady-flow case with a stationary wave oriented normal to the flow. Although our results could be extended in a straightforward way to stationary oblique waves, the main points of our investigation can most readily be seen for the simplest case of waves normal to the flow. The thermodynamic analysis for the unsteady case is discussed elsewhere.¹¹ The present study is also restricted to considering idealized detonations that can be treated through the jump conditions and thermodynamics. We recognize that chemical kinetics, detonation wave structure, and instability are important features of detonations¹² but, in the present study, we focus on the mean flow and thermodynamic aspects; some considerations about stability and wave structure are given by Wintenberger.¹³

We start our discussion by reviewing standard thermodynamic cyclic analysis, focusing on the role of entropy generation in determining efficiency. Next, we consider the conventional Hugoniot analysis, and conclude that this approach is not appropriate for comparing combustion modes for stationary combustion waves in propulsion systems. We propose that in order to compare combustion modes on an equal basis in steady-flow, we need to fix the upstream stagnation state and require that the combustion wave speed be determined so that the wave is always stationary relative to the propulsion system. We reformulate the conventional analysis of steady combustion waves to obtain solutions for a fixed initial stagnation state and conclude that steady detonation waves generate more entropy than steady deflagrations at a given flight condition. In particular, focusing on the irreversible portion of the entropy rise in the combustion process, we demonstrate that it is the irreversibility associated with stationary detonation waves in steady-flow which causes the poor performance of steady detonation-based propulsion.

Thermodynamic cycle analysis

The thermodynamic processes encountered in air-breathing propulsion involve sequential compression, combustion, and expansion. This sequence is turned into a closed cycle through a constant-pressure process during which the fluid exhausted into the atmosphere at the end of the expansion process is converted into the inlet fluid by exchanging heat and work with the surroundings. The thermal efficiency of an arbitrary cycle involving adiabatic combustion can be defined as the ratio of the work done by the system to the heat of combustion of the

fuel-air mixture (on a specific mass basis).

$$\eta_{th} = \frac{w}{q_c} \quad (1)$$

The meaning of work done and mixture heat of combustion can be clarified by considering a thermodynamic cycle consisting of an arbitrary adiabatic process taking the system from its initial state 1 to state 4, and ending with a constant-pressure process taking the system back to state 1. In the present case, the system consists of a fixed mass of working fluid. Between states 1 and 2, the working fluid is a fuel-air mixture. We suppose that an adiabatic combustion process transforms the working fluid from reactants to products between states 2 and 3. The working fluid is combustion products between states 3 and 5. The sequence of states 1-2-3-4 are shown with a dashed line since these processes may involve nonequilibrium states and processes that cannot be represented uniquely in the pressure-volume plane.

Since processes 1-2-3-4 are adiabatic, the heat interactions exist only between states 4-5-1. We will suppose that states 4 and 5 are in chemical and thermal equilibrium and state 1 is a mixture of fuel and air that is in thermal but not chemical equilibrium. As shown in Fig. 1, there is an intermediate state 5 between 4 and 1 that divides the heat interaction into a heat removal (4-5) step and heat addition (5-1) step. The heat interaction between steps 4 and 5 is required to remove an amount of thermal energy $q_{out} > 0$ from the products of combustion and cool the flow down from the exhaust temperature to the ambient conditions. Since this process occurs at constant pressure, the First Law of Thermodynamics determines the heat interaction from the enthalpy change

$$q_{out} = h_4 - h_5 . \quad (2)$$

The heat interaction between steps 5 and 1 is required to add an amount of thermal energy $q_{in} > 0$ in order to convert the combustion products back to reactants. The First Law of Thermodynamics can again be used to compute the heat interaction from the enthalpy change

$$q_{in} = h_1 - h_5 . \quad (3)$$

Note that this defines the quantity $q_c = q_{in}$ in a fashion consistent with standard thermochemical practice if the ambient conditions correspond to the thermodynamic standard state. Applying the First Law of Thermodynamics around the cycle, the work done by the system can be computed as the net heat interaction

$$w = q_{in} - q_{out} = h_1 - h_4 . \quad (4)$$

The thermal efficiency (Eq. 1) can, therefore, be rewritten as

$$\eta_{th} = \frac{h_1 - h_4}{h_1 - h_5} = \frac{h_1 - h_4}{q_c} . \quad (5)$$

For steady-flow engines, the cycle analysis based on a closed system (fixed mass of material) is completely equivalent to the flow path analysis based on an open system, as long as the mass and momentum contributions of the fuel are negligible and the exhaust flow is fully expanded at the exit plane.³ Within these assumptions, we can make a correspondence between states in the cyclic process of Fig. 1 and an open thermodynamic cycle. If the states in the open and closed cycles are equivalent, then the thermal efficiencies are the same for the two processes. The precise equivalence is based on the control volume analysis of the energy balance in an open system whose inlet plane is at state 1 and exit plane is at state 4. For an adiabatic open system with no work interaction, the energy balance between the inlet and exit for a quasi-one dimensional system¹⁴ yields

$$h_1 + u_1^2/2 = h_4 + u_4^2/2 . \quad (6)$$

Using the cycle thermal efficiency as defined in Eq. 1, we find that

$$\eta_{th} = \frac{u_4^2 - u_1^2}{2q_c} . \quad (7)$$

Based on this equivalence, the thrust of a steady pressure-matched propulsion system can be directly calculated from the thermal efficiency.³

$$F = \dot{m}_1 (u_4 - u_1) = \dot{m}_1 \left(\sqrt{u_1^2 + 2\eta_{th}q_c} - u_1 \right) \quad (8)$$

This is the key link between ideal steady-flow propulsion system performance and thermodynamic cycle analysis. For steady flows, thermodynamic analysis of an idealized cycle is used to compute the efficiency through Eq. 5 and then the thrust can be computed by equating this to the efficiency defined by Eq. 7.

For an ideal (reversible) process, the heat removed during the constant-pressure process 4–5 can be expressed as

$$q_{out} = \int_{s_5}^{s_4} T ds \quad (9)$$

and the thermal efficiency is

$$\eta_{th} = 1 - \frac{\int_{s_5}^{s_4} T ds}{q_c} . \quad (10)$$

For a given initial state 1 and a given mixture, state 5 is fixed and the value of the entropy is determined by the specific heat of combustion and the product and reactant composition. Thus, the heat removed q_{out} increases and the thermal efficiency decreases with increasing values of s_4 . In general, the thermal efficiency is maximized when the entropy rise during process 1–4 is minimized.

This general result can be computed explicitly if we consider a perfect gas and take $s_5 = s_1$, which is approximately satisfied for real mixtures and exactly so for the simple model discussed later in this paper. The integral of Eq. 9 is calculated explicitly as a function of the entropy rise between states 1 and 4, and the thermal efficiency becomes

$$\eta_{th} = 1 - \frac{C_p T_1}{q_c} \left[\exp \left(\frac{s_4 - s_1}{C_p} \right) - 1 \right]. \quad (11)$$

Another approach highlighting the role of entropy generation in a steady-flow system is to consider the flow availability. The flow availability per unit mass is defined relative to the environment at pressure P_0 and temperature T_0 as the maximum theoretical work obtainable as the flow is brought to equilibrium with the environment.

$$a_f = h - h_0 - T_0(s - s_0) + u^2/2 \quad (12)$$

Note that the values of h_0 and s_0 are different for reactants and products. The availability balance between the inlet and exit planes of a single-stream, steady-flow, adiabatic system is

$$\dot{m}(a_{f4} - a_{f1}) = \dot{w}_{ideal} - T_0 \dot{P}_s \quad (13)$$

where $\dot{w}_{ideal} = \dot{m} [h_0^r - h_0^p - T_0(s_0^r - s_0^p)]$ is the ideal work per unit time that can be obtained from the conversion of reactants into products at environment conditions. The Second Law of Thermodynamics states that the entropy generation per unit time $\dot{P}_s = \dot{m}(s_4 - s_1) \geq 0$. Thus, it is clear from Eq. 13 that the entropy generation between states 1 and 4 reduces the increase in flow availability from its maximum value and, therefore, the propulsive power.¹⁵

The overall entropy rise is the sum of the entropy rise generated by combustion and of the entropy increments generated by irreversible processes such as shocks, friction, heat transfer, Rayleigh losses (combustion or equivalent heat addition at finite Mach number), or fuel-air mixing.³ A portion of the entropy increment generated by the combustion process is associated with the fact that the temperature increases significantly in combustion, analogous to the entropy increase that is produced by a reversible addition of heat to a non-flowing system. However, this entropy increment also has an irreversible component, which depends on the combustion mode.

The thermodynamic cycle analysis of this section points to the key role of entropy generation in determining cycle efficiency and propulsion performance. In the following sections, we will focus on determining the entropy generation involved in various combustion modes. Once the entropy change in the combustion process is computed, we can use either Eq. 10 or 11 to determine the efficiency from the entropy change and Eq. 8 to find the propulsion system performance. Applications of this method to model systems involving detonation and deflagration combustion modes are given by Wintenberger.^{8,13}

Entropy variation along the Hugoniot

In this section, we supply the well-known and basic facts regarding the elementary gas dynamics and thermodynamics of detonation waves considered as discontinuities. The different steady combustion modes that can be obtained are usually analyzed using a control volume surrounding the combustion wave, such as that of Fig. 2. The mass, momentum, and energy conservation equations¹⁴ for an idealized, one-dimensional wave with no storage in the control volume and or diffusive transport at the control volume boundaries are

$$\rho_1 u_1' = \rho_2 u_2' , \tag{14}$$

$$P_1 + \rho_1 u_1'^2 = P_2 + \rho_2 u_2'^2 , \tag{15}$$

$$h_1 + u_1'^2/2 = h_2 + u_2'^2/2 . \tag{16}$$

States 1 and 2 correspond respectively to the reactants upstream of the wave and the products downstream of the wave. The upstream state composition is specified and the downstream state composition is determined by requiring that the products are in chemical equilibrium. The equation of state for the products must also be specified to complete the description. For the cases we consider, the ideal gas equation of state and tabulated thermodynamic properties are the appropriate level of description. The usual analysis considers fixed thermodynamic conditions upstream (P_1, ρ_1, h_1) and a variable inflow velocity u_1' . Although this is the conventional approach, as we will see later, it is not the most appropriate approach for optimizing steady, air-breathing propulsion systems.

The Hugoniot curve determines the locus of the possible solutions for state 2 from a given state 1 and a given energy release q_c . In particular, it is instructive to plot the Hugoniot on a pressure-specific volume diagram (Fig. 3). The dashed portion of the curve labeled “forbidden” is physically impossible for Rayleigh processes.² The solutions located in the upper branch of the Hugoniot are supersonic waves (detonations), whereas the solutions located in the lower branch are subsonic waves (deflagrations).

The points where the Rayleigh line is tangent to the Hugoniot curve are called the

Chapman-Jouguet (CJ) points.² The CJ points are characterized by sonic flow downstream of the combustion wave and correspond to entropy extrema of the burned gases. It is possible to show, based on the curvature of the Hugoniot curve,² that the entropy is minimum at the upper CJ point and maximum at the lower CJ point (Fig. 4). The CJ points divide the possible locus of solutions into four regions, corresponding to strong detonations (supersonic flow to subsonic), weak detonations (supersonic to supersonic), weak deflagrations (subsonic to subsonic), and strong deflagrations (subsonic to supersonic). Strong deflagrations and weak detonations can be ruled out except in extraordinary situations by considering the reaction zone structure.² The physically acceptable and observed solutions for steady waves are weak deflagrations and strong detonations. The solution to Eqs. 14–16 is uniquely determined only with some additional considerations. For deflagrations, the structure of the combustion wave and turbulent and diffusive transport processes determine the actual propagation speed. For detonations, gas dynamic considerations are apparently sufficient to determine the propagation speed (corresponding to the CJ_U solution), independent of the actual structure of the wave.² Strong detonations are observed only in the transient state or if there is an “effective” piston created by the flow following the wave.

We now consider the case of the perfect gas $P = \rho RT$ in order to numerically illustrate the previous points. We will assume equal specific heat capacities for reactants and products

$$C_p = \frac{\gamma}{\gamma - 1}R \quad (17)$$

and the enthalpy in the reactants and products can be expressed as

$$h_1 = C_p T_1 \quad h_2 = C_p T_2 - q_c . \quad (18)$$

The set of Eqs. 14–16 can be rewritten for a perfect gas as a function of the Mach numbers upstream and downstream of the wave.

$$\frac{\rho_2}{\rho_1} = \frac{M_1^2(1 + \gamma M_2^2)}{M_2^2(1 + \gamma M_1^2)} \quad (19)$$

$$\frac{P_2}{P_1} = \frac{1 + \gamma M_1^2}{1 + \gamma M_2^2} \quad (20)$$

$$\frac{q_c}{C_p T_1} + 1 + \frac{\gamma - 1}{2} M_1^2 = \frac{M_2^2(1 + \gamma M_1^2)^2}{M_1^2(1 + \gamma M_2^2)^2} \left(1 + \frac{\gamma - 1}{2} M_2^2 \right) \quad (21)$$

This set of equations can be solved analytically for a given q_c and initial state and the resulting Hugoniot for the perfect gas is given in Fig. 3. Note that the solution curves shown in Figs. 3 and 4 are parameterized by M_1 . Each point on the curve corresponds to a different

combustion wave speed and requirements for combustor design.

The entropy rise associated with the combustion process can be computed from Eqs. 19 and 20.

$$\frac{s_2 - s_1}{R} = \frac{\gamma}{\gamma - 1} \ln \left(\frac{T_2}{T_1} \right) - \ln \left(\frac{P_2}{P_1} \right) \quad (22)$$

The entropy rise is plotted in Fig. 4 as a function of the specific volume. The different solution regions are shown and the entropy rise has a global minimum at the CJ detonation point and a global maximum at the CJ deflagration point. Thus, from Eq. 11, it appears as if a cycle using detonation combustion will yield the highest thermal efficiency since it has the lowest entropy rise.

The role of irreversibility in steady-flow propulsion

The fact that the entropy rise is minimum at the CJ detonation point, in conjunction with the result of Eq. 10, has motivated several efforts to explore stationary detonation applications to steady-flow propulsion.⁶⁻⁸ However, these studies concluded that the performance of steady detonation-based engines is always substantially lower than that of the ramjet. The explanation of this apparent contradiction lies in considering the role of entropy generation and irreversible processes in the combustor. It is a general conclusion of thermodynamics and can be explicitly shown using availability arguments¹⁵ (Eq. 13) that the work obtained is maximized when the irreversibility is minimized. When portions of the propulsion system involve losses and irreversible generation of entropy, the efficiency is reduced and the reduction in performance (specific thrust) can be directly related to the irreversible entropy increase.¹

The entropy rise occurring during premixed combustion in a flowing gas has a minimum component due to the energy release and the chemical reactions, and an additional, irreversible, component due to the finite velocity and, in the case of a detonation, the leading shock wave.

$$s_2 - s_1 = \Delta s_{min} + \Delta s_{irr} \quad (23)$$

For a combustion wave such as that in Fig. 2, we propose that the minimum entropy rise (for a *fixed* upstream state and velocity) can be computed by considering the ideal stagnation or total state.* The total properties at a point in the flow are defined as the values obtained

*This conjecture is easy to demonstrate for a perfect gas with an effective heat addition model of combustion.¹⁶ We also demonstrate the correctness of this idea explicitly in subsequent computations for the one- γ detonation model and numerical solutions with realistic thermochemistry.

by isentropically bringing the flow to rest. For example, the total enthalpy is

$$h_t = h + \frac{u^2}{2} \quad (24)$$

and the total pressure and temperature are defined by

$$h(P_t, s) = h_t \quad h(T_t, s) = h_t, \quad (25)$$

where by definition $s_t = s$. The process of computing the stagnation state is illustrated graphically in the (h,s) or Mollier diagram of Fig. 5. Differentiating Eq. 25 yields

$$dh_t = T_t ds + \frac{1}{\rho_t} dP_t. \quad (26)$$

At fixed total enthalpy, the total pressure decreases with increasing entropy

$$dP_t = -\rho_t T_t ds \quad (27)$$

so that the minimum entropy rise is associated with the highest total pressure, which is the upstream value P_{t1} . This is illustrated graphically in Fig. 5, showing the additional entropy increment Δs_{irr} associated with a total pressure decrement $P_{t1} - P_{t2}$.

For a given stagnation state, the minimum entropy rise can be determined for gas mixtures with realistic thermochemistry by considering an ideal constant-pressure (zero velocity) combustion process. The first step is to determine the total temperature in the products from the energy balance equation

$$h_2(T_{t2}) = h_1(T_{t1}), \quad (28)$$

where the species in state 2 are determined by carrying out a chemical equilibrium computation. The second step is to determine the entropy rise across the combustion wave by using the stagnation pressures, temperatures, and compositions to evaluate the entropy for reactants and products

$$\Delta s_{min} = s_2(T_{t2}, P_{t1}) - s_1(T_{t1}, P_{t1}). \quad (29)$$

The total entropy jump across the wave is

$$s_2 - s_1 = s_2(T_2, P_2) - s_1(T_1, P_1), \quad (30)$$

where state 2 in the products is determined by solving the jump conditions. The irreversible

component can then be computed by using Eq. 23.

For a perfect gas model, the entropy change can be explicitly computed as

$$s_2 - s_1 = C_p \ln \left(\frac{T_{t2}}{T_{t1}} \right) - R \ln \left(\frac{P_{t2}}{P_{t1}} \right) . \quad (31)$$

From Eq. 29, the minimum entropy rise is

$$\Delta s_{min} = C_p \ln \left(\frac{T_{t2}}{T_{t1}} \right) \quad (32)$$

and the irreversible component is

$$\Delta s_{irr} = -R \ln \left(\frac{P_{t2}}{P_{t1}} \right) . \quad (33)$$

The minimum component can be identified as the amount of entropy increase that would occur with an equivalent *reversible* addition of heat

$$ds = \frac{dq}{T} \quad (34)$$

at constant pressure, for which

$$dq = dh = C_p dT . \quad (35)$$

Substituting and integrating from stagnation state 1 to 2, we find that

$$\Delta s_{rev} = C_p \ln \left(\frac{T_{t2}}{T_{t1}} \right) , \quad (36)$$

which is identical to the expression for the minimum entropy rise found from evaluating the entropy change using the prescription given above. Using these definitions, we show in Fig. 6 the partition of the entropy into these two portions for the perfect gas case considered earlier.

Although the total entropy rise is lower for the detonation branch than the deflagration branch, a much larger portion (greater than 50%) of the entropy rise is irreversible for detonations than for deflagrations (less than 5%). Separate computations show that the majority of the irreversible portion of the entropy rise for detonations is due to the entropy jump across the shock front, which can be obtained directly from the total pressure decrease across the shock wave and Eq. 31. This loss in total pressure is orders of magnitude larger for detonation than for deflagration solutions and has been shown⁶ to be responsible for the lower performance of detonation-based engines relative to the ramjet. Hence, the paradox

mentioned earlier can be resolved by considering not just the total entropy rise, but by determining what part of this is irreversible. An alternative way to look at this issue is given in the next section, where we reformulate the jump conditions so that the role of irreversible entropy rise in the calculation of the thermal efficiency can be demonstrated explicitly.

Irreversible entropy rise and thermal efficiency

The role of the irreversible part of the entropy rise can be explored further by considering Eq. 10. In order to compare objectively different combustion modes, the engine has to be studied in a given flight situation for a fixed amount of energy release during the combustion, as shown in Fig. 7. Our conceptual engine consists of an inlet, a combustion chamber with a steady combustion wave, and a nozzle. State 0 corresponds to the freestream conditions, while state 1 denotes the state of the flow just upstream of the combustion wave; state 2 is the state just downstream of the combustion wave, and state e corresponds to the conditions at the exit plane of the engine. The conditions for combustion wave stabilization are not considered in our thermodynamic analysis. We only require that the wave be stationary, i.e., the flow Mach number just upstream of the combustion wave has to equal the wave propagation Mach number.

From a reference frame fixed relative to the engine, the boundary conditions upstream of the engine consist of air at fixed outside conditions (pressure P_0 and temperature T_0) flowing into the engine at a fixed velocity equal to the flight velocity u_0 , as depicted in Fig. 7. These boundary conditions correspond to a single value of the total enthalpy $h_{t0} = h(T_0, P_0) + u_0^2/2$ and of the entropy $s_0 = s(T_0, P_0)$. Thus, they determine a single freestream stagnation state defined by the set of stagnation properties h_{t0} and $P_{t0} = P(h_{t0}, s_0)$. However, the static conditions just upstream of the combustion wave vary with the combustion mode and its associated propagation Mach number. Hence, fixed static conditions upstream of the combustion wave are not representative of actual flight situations and the conventional Hugoniot analysis, which is based on this assumption, can be misleading when trying to compare the relative merits of various combustion modes. At a given flight condition, the static conditions ahead of a stationary wave will be different for different combustion modes and the common factor will instead be the freestream stagnation state (h_{t0}, P_{t0}) .

The entropy rise between the inlet and exit planes is the sum of the entropy rise through the combustion and the irreversible entropy increments through the inlet and nozzle. Grouping together the irreversible entropy increments through the inlet, the combustion chamber, and the nozzle,

$$s_e - s_0 = \Delta s_{min} + \Delta s_{irr} . \tag{37}$$

The minimum part of the entropy rise during combustion is constant for a fixed energy

release and a fixed stagnation state upstream of the wave. From the general principles of thermodynamics and consistent with Eq. 10, the highest efficiency is obtained with the minimum irreversibility for a given chemical energy release q_c .

This general statement can be shown explicitly for the case of the perfect gas. Using the one- γ model of detonations,¹⁴ the energy equation is expressed as

$$C_p T_{t2} = C_p T_{t1} + q_c . \quad (38)$$

Combining Eq. 32 with the previous expression, the minimum component of the entropy rise for the one- γ model of detonations¹⁴ is

$$\Delta s_{min} = C_p \ln \left(1 + \frac{q_c}{C_p T_{t1}} \right) . \quad (39)$$

Substituting Eq. 37 into Eq. 11, and using the result of Eq. 39, the thermal efficiency can be expressed as a function of the irreversible entropy rise

$$\eta_{th} = 1 - \frac{C_p T_0}{q_c} \left[\left(1 + \frac{q_c}{C_p T_{t1}} \right) \exp \left(\frac{\Delta s_{irr}}{C_p} \right) - 1 \right] . \quad (40)$$

Note that T_0 in this expression corresponds to T_1 used in Eq. 11 since in the present section we are using T_1 for the variable state just upstream of the wave. From Eq. 40, the highest efficiency is obtained for $\Delta s_{irr} = 0$

$$\eta_{th} < \eta_{th}(\Delta s_{irr} = 0) = 1 - \frac{T_0}{T_{t1}} , \quad (41)$$

which is the classical expression for the ideal Brayton cycle.

Consider an idealized version of our conceptual engine, for which the thermal efficiency is determined only by the irreversible entropy rise during combustion. In order to compare different combustion modes, we need to calculate the irreversible entropy rise for all the possible solutions to Eqs. 14–16. However, the result of Fig. 4 does not apply directly because the velocity of the initial state and, consequently, the total enthalpy are not constant for the conventional Hugoniot analysis. Instead, it is necessary to compute another solution curve corresponding to a fixed freestream stagnation state, which we will refer to as the stagnation Hugoniot.

The stagnation Hugoniot

The stagnation Hugoniot is the locus of the solutions to the conservation equations (Eqs. 14-16) for a given stagnation state upstream of the combustion wave. The stagna-

tion Hugoniot analysis considers fixed total enthalpy h_{t1} and entropy s_1 . The flow properties upstream of the combustion wave vary with inflow velocity u'_1 .

$$h_1 = h_{t1} - u'_1{}^2/2 \quad (42)$$

$$P_1 = P(h_1, s_1) \quad (43)$$

$$v_1 = v(h_1, s_1) \quad (44)$$

All the solution states to the stagnation Hugoniot can be found by varying the inflow velocity. Varying the inflow velocity modifies the state 1 just upstream of the combustion wave. We will refer to the *local* Hugoniot analysis as the conventional Hugoniot analysis for a given constant state 1 defined by a value of the inflow velocity along the stagnation Hugoniot. The general properties of the stagnation Hugoniot can be deduced from the classical results for the conventional Hugoniot.²

Like in the conventional Hugoniot analysis, the inflow velocity has a minimum value along the detonation branch and a maximum value along the deflagration branch (Fig. 8). We show that these points correspond to the CJ conditions. The inflow velocity is related to the pressure and volume across the combustion wave through the Rayleigh line relationship.

$$u'_1{}^2 = -v_1^2 \cdot \frac{P_2 - P_1}{v_2 - v_1} \quad (45)$$

Differentiating this equation, and keeping in mind that the properties at state 1 also vary,

$$du'_1{}^2 = -\frac{v_1^2}{(v_2 - v_1)^2} [(2v_2/v_1 - 1)(P_2 - P_1)dv_1 - (v_2 - v_1)dP_1 + (v_2 - v_1)dP_2 - (P_2 - P_1)dv_2] . \quad (46)$$

At the inflow velocity extrema (i.e., $du'_1 = 0$), we have from Eq. 42 that $dh_1 = -u'_1 du'_1 = 0$ and since the entropy at state 1 is given, $dP_1 = dh_1/v_1 = 0$ and $dv_1 = 0$. Thus, these points also correspond to extrema of enthalpy, pressure, and specific volume at state 1. Simplifying all the differentials vanishing at the inflow velocity extrema, Eq. 46 holds only if

$$\frac{\partial P_2}{\partial v_2} = \frac{P_2 - P_1}{v_2 - v_1} , \quad (47)$$

which means that, for the upstream states corresponding to inflow velocity extrema, the local Hugoniot and the Rayleigh line are tangent. Thus, the points at which the inflow velocity has an extremum are CJ points.

From the conventional Hugoniot analysis, we know that the entropy along the local Hugoniot has an extremum at the CJ points,² i.e. $\partial s_2/\partial v_2 = 0$. This result is straightforward

to extend to the stagnation Hugoniot.

$$\frac{\partial s_2}{\partial u'_1} = \frac{\partial s_2}{\partial v_2} \cdot \frac{\partial v_2}{\partial u'_1} = 0 \quad (48)$$

Additionally, it can be shown that

$$\frac{\partial^2 s_2}{\partial u'^2_1} = \frac{\partial^2 s_2}{\partial v^2_2} \left(\frac{\partial v_2}{\partial u'_1} \right)^2. \quad (49)$$

Based on the local Hugoniot analysis,² we know that $\partial^2 s_2 / \partial v^2_2 \geq 0$ at the CJ detonation point. Thus, the entropy along the stagnation Hugoniot is minimum at the CJ detonation point, and, conversely, maximum at the CJ deflagration point. Because the detonation and deflagration branches are disjoint, as we will see next, these are only local extrema. We now calculate the stagnation Hugoniot for the perfect gas case and carry numerical solutions for a case with realistic thermochemistry.

Stagnation Hugoniot for the perfect gas

We compute the stagnation Hugoniot for a perfect gas, based on Eqs. 19–21. Equation 21 has to be rewritten as a function of the parameter $q_c / C_p T_{t1}$, which has a fixed value for a given freestream condition.

$$1 + \frac{q_c}{C_p T_{t1}} = \frac{M_2^2 (1 + \gamma M_1^2)^2 (1 + \frac{\gamma-1}{2} M_2^2)}{M_1^2 (1 + \gamma M_2^2)^2 (1 + \frac{\gamma-1}{2} M_1^2)} \quad (50)$$

This equation can be solved analytically for M_2 as a function of M_1 . The solution curves shown in Figs. 9 and 10 can be obtained by parametric (M_1 being the parameter) evaluation of Eqs. 19–21 or else as shown in the Appendix, as explicit solutions in terms of v_2 / v_1 . Detonation solutions are found to be possible only for

$$\frac{q_c}{C_p T_{t1}} < \frac{1}{\gamma^2 - 1}. \quad (51)$$

This condition is imposed by the requirement that $T_1 > 0$ and is in agreement with our results on detonation ramjets⁸ using a simple one- γ detonation model.¹⁴ For higher values of $q_c / C_p T_{t1}$, the total enthalpy is not high enough to enable a steady detonation in the combustor for the given value of the heat release, and no steady solutions exist.

For the conventional Hugoniot (Fig. 3), the entropy, pressure, and temperature at state 2 are finite for a constant-volume ($v_2 = v_1$) explosion process even though, in this limit, $M_1 \rightarrow \infty$. However, in the stagnation Hugoniot representation, the pressure ratio along

the weak detonation branch becomes infinite as this limit is approached. As $M_1 \rightarrow \infty$, M_2 asymptotes to a constant value instead of becoming infinite as for the conventional Hugoniot.

$$M_2 \rightarrow \sqrt{\frac{1 - (\gamma - 1)\frac{q_c}{C_p T_{t1}} + \sqrt{1 - (\gamma^2 - 1)\frac{q_c}{C_p T_{t1}}}}{\gamma(\gamma - 1)\frac{q_c}{C_p T_{t1}}}} \quad (52)$$

This is due to the fact that the stagnation conditions at state 2 are fixed by the stagnation conditions at state 1 and the heat release. As $M_1 \rightarrow \infty$, the static pressure at state 1 decreases towards zero because the total pressure is fixed, but the static pressure at state 2 remains finite due to the finite value of M_2 . This explains the unusual shape of the stagnation Hugoniot, which is plotted in the pressure-specific volume plane for $\gamma = 1.4$ and $q_c/C_p T_{t1} = 0.8$ in Fig. 9. Just as for the conventional Hugoniot, there is no solution in the positive quadrant of the pressure-specific volume plane for Rayleigh processes. However, unlike the conventional Hugoniot, the stagnation Hugoniot curve is not continuous across this forbidden region. This means that the detonation and deflagration branches are disjoint.

The total entropy rise along the stagnation Hugoniot is shown in Fig. 10 as a function of the specific volume ratio. For a fixed heat release and initial stagnation state, the minimum entropy rise is constant (Eq. 39) and the variation of the total entropy rise is caused by the change in irreversible entropy rise associated with the combustion mode. As in the conventional Hugoniot, the CJ points correspond to extrema of the entropy. However, they are only local extrema because of the discontinuity of the solution curve in the pressure-specific volume plane. The CJ detonation point corresponds to a minimum in entropy along the detonation branch, while the CJ deflagration point corresponds to a maximum in entropy along the deflagration branch. However, the entropy rise associated with the CJ detonation point is much larger than that associated with the CJ deflagration point for all possible values of $q_c/C_p T_{t1}$. In general, the irreversible entropy rise associated with any physical solution on the deflagration branch is much lower than that for any detonation solution. Of all physically possible steady combustion modes, constant-pressure (CP) combustion at zero Mach number is the process with the smallest entropy rise for a fixed stagnation condition.

The result of Figs. 10 shows explicitly that steady combustion waves with a finite (non-zero) velocity generate irreversible entropy. For deflagrations, this irreversible entropy rise is due to combustion at finite velocity and is responsible for the total pressure losses classically observed for steady combustion at finite Mach number,¹⁶ for example, in ramjets. This effect is also present for detonations, but the presence of the shock wave in detonations contributes to the majority of the irreversible entropy rise.

Stagnation Hugoniot for a gas with realistic thermochemistry

We carried out numerical computations to verify that the results obtained for the perfect gas case extend to the case of a gas with realistic thermochemistry. We developed an numerical procedure using Stanjan¹⁷ to compute the stagnation Hugoniot. The procedure iterates on the wave inflow velocity u'_1 . For a given wave inflow velocity, Stanjan is used to compute a constant-entropy, frozen-composition solution from the stagnation conditions to state 1, whose enthalpy is determined by Eq. 42. Once state 1 is determined, Stanjan is used to compute the equilibrium solutions to the jump conditions (Eqs. 14–16). The procedure consists of using trial values of specific volume for detonation cases and the pressure for deflagration cases, and calculating the other variable using Eq. 45. Based on the trial values upstream of the wave, Stanjan solves for the downstream equilibrium state using a specified pressure, specific volume equilibrium option. The enthalpy obtained from the equilibrium solution is then compared with the enthalpy calculated from the jump conditions (Eq. 16), and the process is iterated until these two values are within a specified tolerance. Convergence is obtained using the bisection method.

The stagnation Hugoniot is plotted in the pressure-specific volume plane of Fig. 11 for a stoichiometric propane-air mixture. The stagnation conditions considered were chosen so that detonation solutions exist (see Eq. 51). The solution curve is similar to that obtained in the perfect gas case and has two disjoint branches corresponding to deflagration and detonation solutions. The total entropy increment, normalized with the initial entropy value, is shown in Fig. 12 as a function of the specific volume ratio. The entropy rise has a local maximum at the CJ deflagration point and a local minimum at the CJ detonation point, but the increment associated with this local minimum is about 40% higher than the value corresponding to the local maximum. Thus, we find that, in the case of a gas with realistic thermochemistry, steady detonation waves generate more entropy than steady deflagrations. We also find that the minimum entropy rise for physically possible solutions is generated by constant-pressure combustion.

Application to steady-flow propulsion systems

We now use the result of Eq. 10 to compare the thermal efficiency of ideal steady propulsion systems as a function of the combustion mode selected. Losses associated with shock waves, friction, mixing, or heat transfer are neglected, and the compression and expansion processes are assumed to be isentropic. The thermal efficiency for an ideal steady propulsion system flying at a Mach number of 5 is plotted in Fig. 13 for a perfect gas. The irreversible entropy rise in detonations strongly penalizes the efficiency of ideal steady detonation-based engines compared to the conventional ideal ramjet. Thus, this approach reconciles flow path

analysis and thermodynamic cycle analysis for detonation-based ramjets. Note that our thermodynamic cycle analysis yields identical results to the flow-path performance analysis of an ideal hydrocarbon-fueled detonation ramjet.⁸ However, the values of the thermal efficiency of Fig. 13 are not representative of practical propulsion systems at a flight Mach number $M_0 = 5$ because the total temperature at the combustor outlet is too high to be sustained by the chamber walls. More realistic studies limit the total temperature at the combustor outlet based on material considerations⁸ and account for additional losses, whose net effect is to significantly decrease the thermal efficiency.⁶

For our ideal propulsion system, the constant-pressure (CP) combustion process yields the highest thermal efficiency of all physical solutions to the conservation equations. Foa¹⁰ concluded that CP combustion was always the optimum solution for steady flow using an argument based on a polytropic approximation of the combustion mode for the perfect gas. We have now extended this result to all physically possible steady combustion modes for the perfect gas and the case of a gas with realistic thermochemistry.

However, in order to compare practical propulsion systems based on different combustion modes, one also has to compute the irreversible entropy rise through the other components of the engine. The entropy rise associated with other irreversible processes such as shocks, friction, mixing, or heat transfer may become significant¹ and dominate the results, particularly at high supersonic flight Mach numbers. These points are important to consider when attempting to compare the merits of a detonation ramjet with a conventional ramjet. In particular, it is not obvious how a detonation ramjet flying near the CJ Mach number (with a minimal entropy rise through the inlet) would compare with a practical ramjet handicapped by a substantial entropy rise caused by the flow deceleration from supersonic to low subsonic velocities through the inlet. However, supersonic mixing in a detonation ramjet will entail an additional entropy rise much larger than that generated by subsonic mixing in the ramjet. Furthermore, the detonation ramjet is limited by condensation and auto-ignition of the fuel-air mixture.⁸ The issues of detonation wave stabilization and its stability in the combustor are still open questions,⁸ and one can speculate that the detonation ramjet might suffer from problems similar to those associated with combustion instabilities in the ramjet.

Conclusions

We have used thermodynamic considerations to investigate the choice of the combustion mode for steady-flow propulsion and its consequence on propulsive performance. We reached the following conclusions:

1. The conventional Hugoniot analysis alone is inappropriate for analyzing the relative merits of steady combustion modes for propulsion.

2. For a given flight condition, the minimum entropy rise associated with combustion is fixed and it is the irreversible component of the overall entropy rise in the system that determines the performance.
3. We reformulated the conventional analysis of steady combustion waves to obtain solutions for a fixed initial stagnation state. We propose that the stagnation Hugoniot analysis is the appropriate method for comparing combustion modes for a given flight condition.
4. For a given upstream stagnation state, steady detonation waves generate a higher entropy rise along the stagnation Hugoniot than deflagration waves, which makes them less desirable for propulsion applications. These findings reconcile thermodynamic cycle analysis with flow path performance analysis of detonation-based ramjets.⁶⁻⁸
5. For a given upstream stagnation state, the combustion process generating the lowest entropy increment on the stagnation Hugoniot is constant-pressure combustion, corresponding to the ideal Brayton cycle.

This paper provides a framework under which all steady combustion modes can be directly compared for propulsion applications. In order to determine the overall performance of a system, one has to perform a detailed engineering analysis taking into account the entropy increments associated with combustion, shocks, mixing, viscous effects, and heat transfer. Our analysis singles out the entropy component associated with the combustion wave and can be used to estimate the contribution of the combustion process to the propulsive performance.

Acknowledgements

This work was supported by Stanford University Contract PY-1905 under Dept. of Navy Grant No. N00014-02-1-0589 Pulse Detonation Engines: Initiation, Propagation, and Performance. We thank the reviewers for their constructive suggestions, particularly the encouragement of the development and inclusion of the explicit relationships given in the Appendix.

Appendix - Explicit Solutions for the Perfect Gas Model

Solutions for the stagnation Hugoniot that are explicit in specific volume can be obtained by algebraic manipulation of the conservation relations (Eqs. 14-16) in the case of a perfect gas with constant specific heats and a fixed heat release as specified in Eqs. 17 and 18. This model can not accurately approximate both reactants and products with common values of γ and R , but is often used to illustrate the qualitative behavior of real gases. In this

spirit, we have provided explicit solutions for this model. We emphasize that for the case of propane-air mixtures (Figs. 8, 11, 12) we have not relied on these solutions but have used numerical solutions of the conservation relations with realistic thermochemical states and species to compute equilibrium in the products.

The perfect gas version of the velocity-volume relationship shown graphically in Fig. 8 is analytically expressed as

$$\frac{u_1'^2}{2C_p T_{t1}} = \frac{1 + \frac{q_c}{2C_p T_{t1}} - \frac{v_2}{v_1}}{\frac{\gamma + 1}{\gamma - 1} \left(1 - \frac{v_2}{v_1}\right) \frac{v_2}{v_1}}. \quad (53)$$

There are some limitations on the values that the specific volume ratio can assume due to the physical constraints on the conditions upstream of the wave. The temperature upstream of the wave is given by the stagnation enthalpy relationship (Eq. 42) as

$$\frac{T_1}{T_{t1}} = 1 - \frac{u_1'^2}{2C_p T_{t1}}. \quad (54)$$

The temperature must be positive and by definition, the kinetic energy of the flow must also be positive so that

$$0 \leq \frac{u_1'}{\sqrt{2C_p T_{t1}}} \leq 1 \quad (55)$$

which limits the range of v_2/v_1 to

$$0 < (v_2/v_1)_1 \leq v_2/v_1 \leq (v_2/v_1)_2 < 1 \quad \text{Detonation branch,} \quad (56)$$

$$1 < (v_2/v_1)_3 \leq v_2/v_1 < \infty \quad \text{Deflagration branch.} \quad (57)$$

The limiting volume ratios $(v_2/v_1)_1$ and $(v_2/v_1)_2$ on the detonation branch can be found by setting the velocity in Eq. 53 to the maximum value $u_1' = \sqrt{2C_p T_{t1}}$. Solving the resulting quadratic equation, we find that

$$(v_2/v_1)_{\frac{1}{2}} = \frac{\gamma}{\gamma + 1} \mp \sqrt{\left(\frac{\gamma}{\gamma + 1}\right)^2 - \frac{\gamma - 1}{\gamma + 1} \left(1 + \frac{q_c}{C_p T_{t1}}\right)}. \quad (58)$$

The lower limit on the deflagration branch $(v_2/v_1)_3$ can be found by setting $u_1' = 0$.

$$(v_2/v_1)_3 = 1 + \frac{q_c}{C_p T_{t1}} \quad (59)$$

The CJ points can also be determined by finding the minimum (detonation branch) and maximum (deflagration branch) velocity points on each branch of the solution. The location

of the CJ points is given by

$$(v_2/v_1)_L^U = \left(1 + \frac{q_c}{C_p T_{t1}}\right) \mp \sqrt{\left(1 + \frac{q_c}{C_p T_{t1}}\right)^2 - \left(1 + \frac{q_c}{C_p T_{t1}}\right)} \quad (60)$$

where U indicates the upper (detonation) and L is the lower (deflagration) CJ point. For the case shown in Figs. 9 and 10 the computed values of the critical volume ratios are given in Table 1.

The pressure-volume relationship shown in Fig. 9 can be obtained as an analytic expression by substituting the velocity-volume relationship given above into the analog of the Rayleigh line (resulting from combining momentum and mass conservation) to obtain

$$\frac{P_2}{P_1} = 1 + \frac{2\gamma}{\gamma - 1} \left(1 - \frac{v_2}{v_1}\right) \left[\frac{1 + \frac{q_c}{C_p T_{t1}} - \frac{v_2}{v_1}}{\frac{\gamma + 1}{\gamma - 1} \left(1 - \frac{v_2}{v_1}\right) \frac{v_2}{v_1} + \frac{v_2}{v_1} - \left(1 + \frac{q_c}{C_p T_{t1}}\right)} \right]. \quad (61)$$

This is the analog of the usual detonation Hugoniot or detonation adiabat.

The entropy-volume relationship shown in Fig. 10 can be obtained as an analytic expression from Eq. 22 where the pressure ratio is given by Eq. 61 and the temperature ratio can be computed explicitly as a function of volume from $T_2/T_1 = P_2/P_1 \cdot v_2/v_1$. The entropy change predicted by this relationship actually becomes negative on the deflagration branch at sufficiently large specific volumes, $v_2/v_1 > (v_2/v_1)_{max} \approx 9.25$ for the case shown in Fig. 10. This results in a further limitation on the admissible values of v_2/v_1 . As mentioned previously, deflagration solutions with $v_2/v_1 > (v_2/v_1)_{CJ, L}$ and detonation solutions with $v_2/v_1 > (v_2/v_1)_{CJ, U}$ are considered² nonphysical in nature. For this reason, the physically acceptable ranges of volumes v_2/v_1 in the stagnation Hugoniot analysis are smaller than given by Eqs. 56-57 and are restricted to

$$(v_2/v_1)_1 \leq v_2/v_1 \leq (v_2/v_1)_{CJ, U} \quad \text{Detonation branch,} \quad (62)$$

$$(v_2/v_1)_3 \leq v_2/v_1 < (v_2/v_1)_{CJ, L} \quad \text{Deflagration branch.} \quad (63)$$

References

¹Riggins, D. W., McClinton, C. R., and Vitt, P. H., "Thrust Losses in Hypersonic Engines Part 1: Methodology," *Journal of Propulsion and Power*, Vol. 13, No. 2, 1997, pp. 281–287.

²Courant, R. and Friedrichs, K. O., *Supersonic Flow and Shock Waves*, Interscience Publishers, Inc., New York, 1967, Chap. 3, pp. 204–235.

³Foa, J. V., *Elements of Flight Propulsion*, John Wiley & Sons, New York, 1960, Chap. 13, pp. 274–287.

⁴Kailasanath, K., “Review of Propulsion Applications of Detonation Waves,” *AIAA Journal*, Vol. 38, No. 9, 2000, pp. 1698–1708.

⁵Heiser, W. H. and Pratt, D. T., “Thermodynamic Cycle Analysis of Pulse Detonation Engines,” *Journal of Propulsion and Power*, Vol. 18, No. 1, 2002, pp. 68–76.

⁶Dunlap, R., Brehm, R. L., and Nicholls, J. A., “A Preliminary Study of the Application of Steady-State Detonative Combustion to a Reaction Engine,” *Jet Propulsion*, Vol. 28, No. 7, 1958, pp. 451–456.

⁷Sargent, W. H. and Gross, R. A., “Detonation Wave Hypersonic Ramjet,” *ARS Journal*, Vol. 30, No. 6, 1960, pp. 543–549.

⁸Wintenberger, E. and Shepherd, J. E., “The Performance of Steady Detonation Engines,” 41st AIAA Aerospace Sciences Meeting and Exhibit, January 6–9, 2003, Reno, NV, AIAA 2003-0714.

⁹Zel’dovich, Y. B., “On the Use of Detonative Combustion in Power Engineering,” *Journal of Technical Physics*, Vol. 10, No. 17, 1940, pp. 1453–1461, in Russian.

¹⁰Foa, J. V., “Single Flow Jet Engines - A Generalized Treatment,” *Journal of the American Rocket Society*, Vol. 21, 1951, pp. 115–126.

¹¹Wintenberger, E. and Shepherd, J. E., “Thermodynamic Analysis of Combustion Processes for Propulsion Systems,” 42nd AIAA Aerospace Sciences Meeting and Exhibit, Jan 5-8, 2004, Reno, NV, AIAA2004-1033.

¹²Fickett, W. and Davis, W. C., *Detonation Theory and Experiment*, Dover Publications Inc., 2001.

¹³Wintenberger, E., *Application of Steady and Unsteady Detonation Waves to Propulsion*, Ph.D. thesis, California Institute of Technology, Pasadena, California, 2004.

¹⁴Thompson, P. A., *Compressible Fluid Dynamics*, Advanced Engineering Series, Rensselaer Polytechnic Institute, 1988, pp. 347–359.

¹⁵Clarke, J. M. and Horlock, J. H., “Availability and Propulsion,” *Journal of Mechanical Engineering Science*, Vol. 17, No. 4, 1975, pp. 223–232.

¹⁶Oates, G. C., *Aerothermodynamics of Gas Turbines and Rocket Propulsion*, AIAA Education Series, 1984, Chap. 2, p. 44.

¹⁷Reynolds, W., “The Element Potential Method for Chemical Equilibrium Analysis: Implementation in the Interactive Program STANJAN,” Tech. rep., Mechanical Engineering Department, Stanford University, 1986.

List of Tables

1	Numerical values corresponding to critical volume ratios for perfect gas stagnation Hugoniot with $\gamma = 1.4$ and $q_c/C_{p1}T_{t1} = 0.8$	25
---	---	----

Table 1: Numerical values corresponding to critical volume ratios for perfect gas stagnation Hugoniot with $\gamma = 1.4$ and $q_c/C_{p1}T_{t1} = 0.8$

$(v_2/v_1)_1$	0.3826
$(v_2/v_1)_{CJ, U}$	0.6000
$(v_2/v_1)_2$	0.7840
$(v_2/v_1)_3$	1.8000
$(v_2/v_1)_{CJ, L}$	3.000

List of Figures

1	Arbitrary thermodynamic cycle ending with constant-pressure process. . . .	27
2	Control volume used to analyze steady combustion waves.	28
3	Hugoniot in the pressure-specific volume plane for a perfect gas with $\gamma=1.4$ and $q_c/C_p T_1=4$	29
4	Variation of the total entropy rise along the Hugoniot for a perfect gas, $\gamma=1.4$, $q_c/C_p T_1=4$	30
5	Mollier diagram used to calculate minimum entropy component. Solid lines are isobars for reactants and dotted lines are isobars for products.	31
6	Minimum and irreversible components of the entropy rise along the Hugoniot for a perfect gas, $\gamma = 1.4$, $q_c/C_p T_1 = 4$	32
7	Ideal steady engine in flight showing the location of the combustion wave. . .	33
8	Inflow velocity along the stagnation Hugoniot for a stoichiometric propane-air mixture. $P_{t1} = 100$ atm, $T_{t1} = 2000$ K, $h_{t1} = 2.113$ MJ/kg.	34
9	Stagnation Hugoniot in the pressure-specific volume plane for a perfect gas with $\gamma = 1.4$ and $q_c/C_p T_{t1} = 0.8$	35
10	Total entropy rise along the stagnation Hugoniot for a perfect gas. The minimum component of the entropy rise is fixed along the stagnation Hugoniot and is shown as the straight line. The total entropy variation is due to the irreversible component only. $\gamma = 1.4$, $q_c/C_p T_{t1} = 0.8$	36
11	Stagnation Hugoniot for a stoichiometric propane-air mixture. $P_{t1} = 100$ atm, $T_{t1} = 2000$ K, $h_{t1} = 2.113$ MJ/kg.	37
12	Total entropy rise along the stagnation Hugoniot for a stoichiometric propane-air mixture. $P_{t1} = 100$ atm, $T_{t1} = 2000$ K, $h_{t1} = 2.113$ MJ/kg, $s_1 = 7.967$ kJ/kgK.	38
13	Thermal efficiency of an ideal engine flying at $M_0 = 5$ as a function of the combustion mode selected for a perfect gas, $\gamma = 1.4$, $q_c/C_p T_{t1} = 0.8$	39

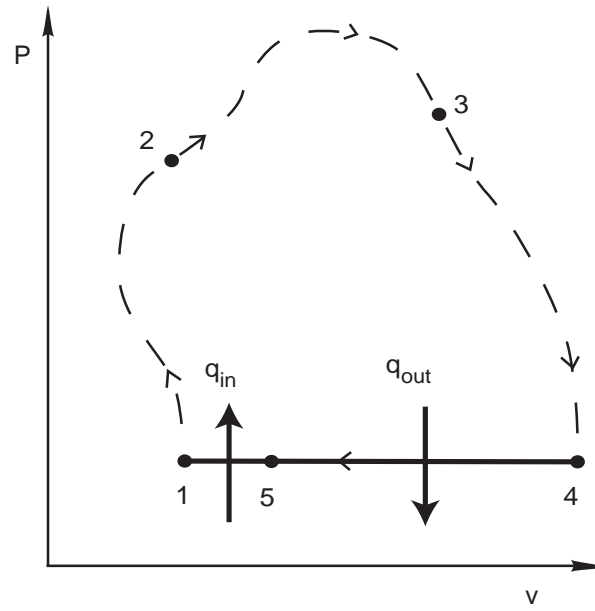


Figure 1: Arbitrary thermodynamic cycle ending with constant-pressure process.

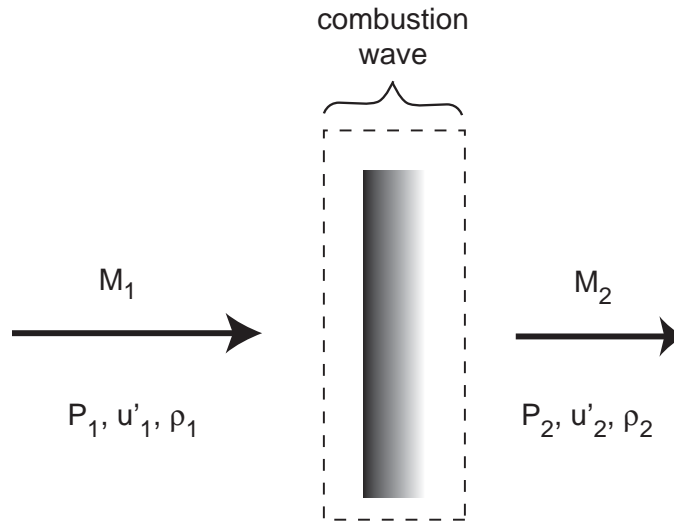


Figure 2: Control volume used to analyze steady combustion waves.

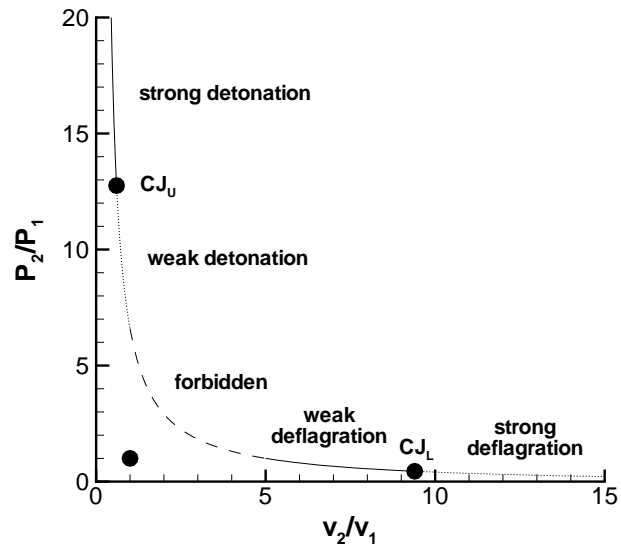


Figure 3: Hugoniot in the pressure-specific volume plane for a perfect gas with $\gamma=1.4$ and $q_c/C_p T_1=4$.

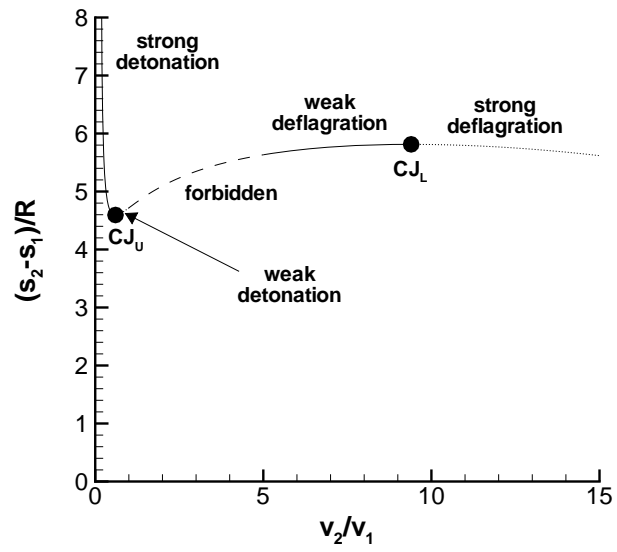


Figure 4: Variation of the total entropy rise along the Hugoniot for a perfect gas, $\gamma=1.4$, $q_c/C_p T_1=4$.

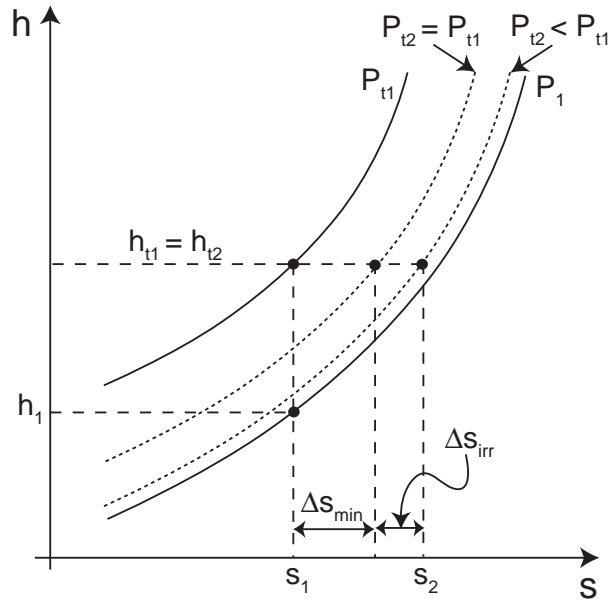


Figure 5: Mollier diagram used to calculate minimum entropy component. Solid lines are isobars for reactants and dotted lines are isobars for products.

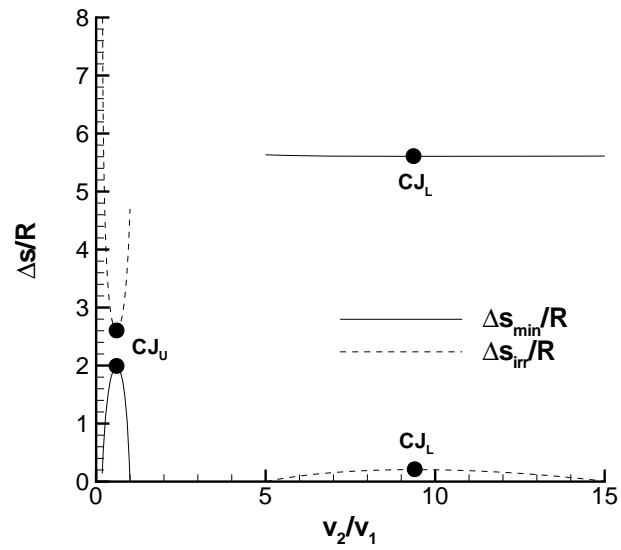


Figure 6: Minimum and irreversible components of the entropy rise along the Hugoniot for a perfect gas, $\gamma = 1.4$, $q_c/C_p T_1 = 4$.

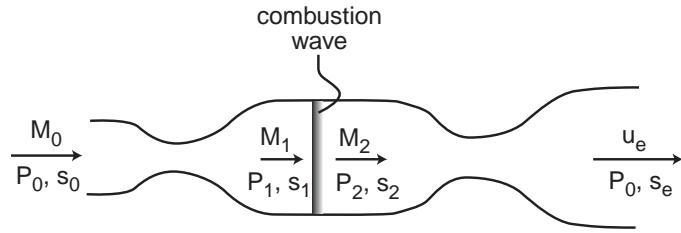


Figure 7: Ideal steady engine in flight showing the location of the combustion wave.

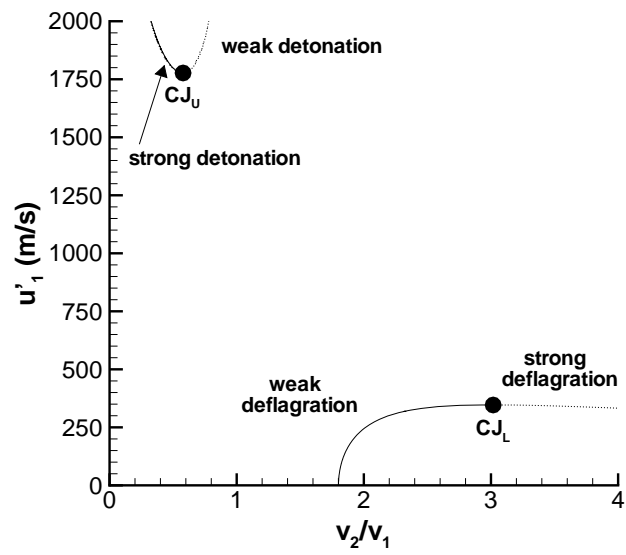


Figure 8: Inflow velocity along the stagnation Hugoniot for a stoichiometric propane-air mixture. $P_{t1} = 100$ atm, $T_{t1} = 2000$ K, $h_{t1} = 2.113$ MJ/kg.

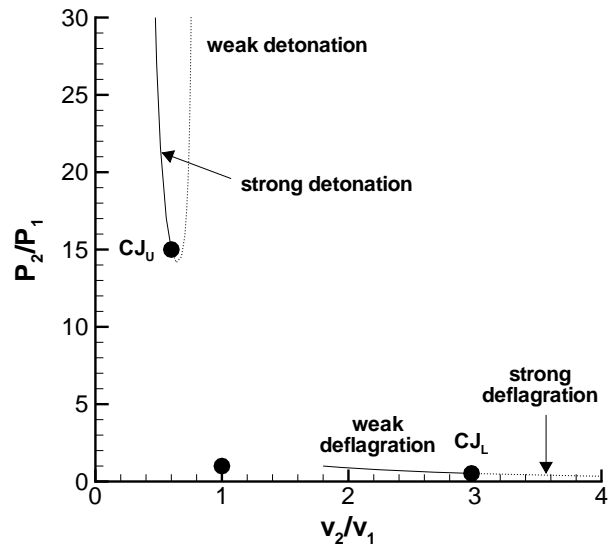


Figure 9: Stagnation Hugoniot in the pressure-specific volume plane for a perfect gas with $\gamma = 1.4$ and $q_c/C_p T_{t1} = 0.8$.

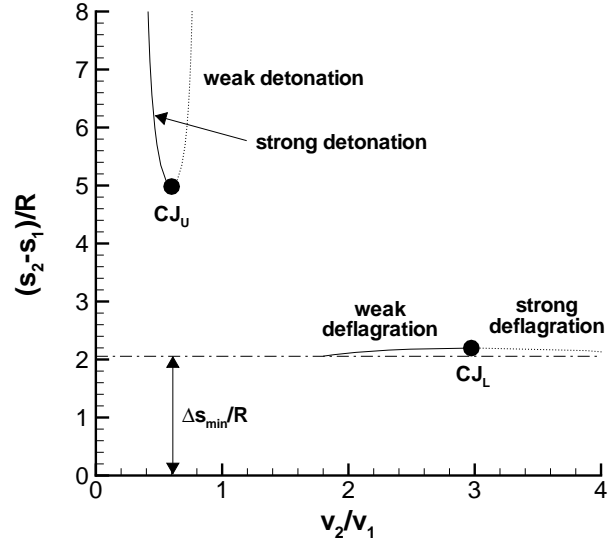


Figure 10: Total entropy rise along the stagnation Hugoniot for a perfect gas. The minimum component of the entropy rise is fixed along the stagnation Hugoniot and is shown as the straight line. The total entropy variation is due to the irreversible component only. $\gamma = 1.4$, $q_c/C_p T_{t1} = 0.8$.

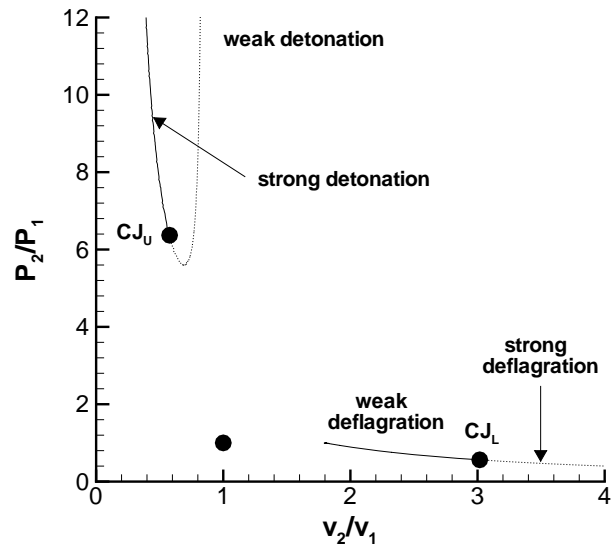


Figure 11: Stagnation Hugoniot for a stoichiometric propane-air mixture. $P_{t1} = 100$ atm, $T_{t1} = 2000$ K, $h_{t1} = 2.113$ MJ/kg.

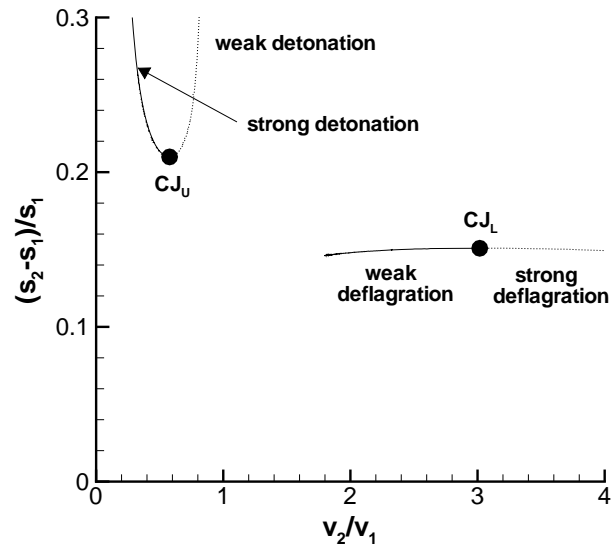


Figure 12: Total entropy rise along the stagnation Hugoniot for a stoichiometric propane-air mixture. $P_{t1} = 100$ atm, $T_{t1} = 2000$ K, $h_{t1} = 2.113$ MJ/kg, $s_1 = 7.967$ kJ/kgK.

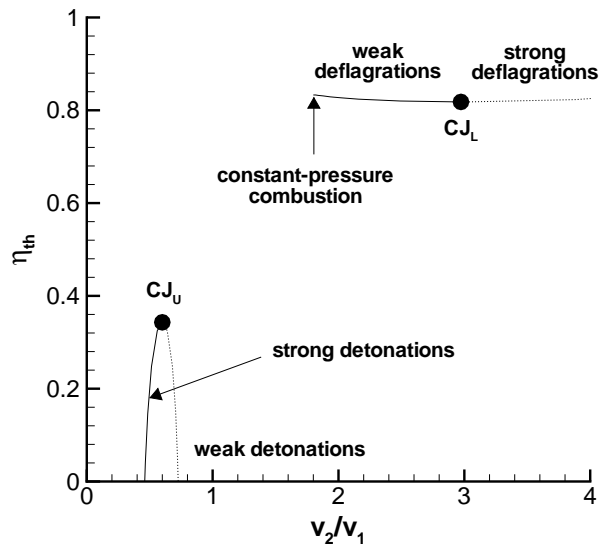


Figure 13: Thermal efficiency of an ideal engine flying at $M_0 = 5$ as a function of the combustion mode selected for a perfect gas, $\gamma = 1.4$, $q_c/C_p T_{t1} = 0.8$.